HHS Public Access

Author manuscript

J Immunol. Author manuscript; available in PMC 2024 June 15.

Published in final edited form as:

J Immunol. 2023 June 15; 210(12): 1889–1898. doi:10.4049/jimmunol.2200659.

The *Tox* gene encodes two proteins with distinct and shared roles in gene regulation

Alyson R. Yeckes[*], **Aaron R. Victor**[*,†], **Zheng Zhu**[*], **Meena Narayanan**[*], **Bharani Srinivasan**[*], **Bethany Bruce**[*], **Jonathan Kaye**[*,‡]

[*]Research Division of Immunology, Department of Biomedical Sciences, Los Angeles, CA 90048

[†]Department of Pathology and Laboratory Medicine, Los Angeles, CA 90048

[‡]Samuel Oschin Comprehensive Cancer Institute, Cedars-Sinai Medical Center, Los Angeles, CA 90048

Abstract

Here we report that the murine *Tox* gene encodes two proteins from a single mRNA and investigate the mechanism of production and function of these proteoforms. The annotated TOX coding sequence is predicted to produce a 526 amino acid protein (TOX_{FL}). However, western blots reveal two bands. We found that the lower band consists of an N-terminally truncated variant of TOX (TOXΔN), while the slower migrating band is TOX_{FL}. The TOXΔN proteoform is alternatively translated via leaky ribosomal scanning from an evolutionarily conserved translation initiation site downstream of the annotated translation initiation site. When expressed exogenously from a cDNA in murine CD8 T cells or HEK cells, or endogenously from the murine *Tox* locus, both forms are translated, although the ratio of TOX_{FL}: TOXΔN significantly varies with cellular context. This includes regulation of proteoform production during development of murine CD4 T cells in the thymus, where the positive selection of $CD4^+8^+$ cells and subsequent differentiation to $CD4^+8^{lo}$ transitional and CD4SP cell subsets is associated with both an increase in total TOX protein and increased TOXΔN production relative to TOX_{FL}. Finally, we found that sole expression of TOX_{FL} had a greater effect on gene regulation during chronic stimulation of murine CD8 T cells in culture mimicking exhaustion, than did TOXΔN, including uniquely regulated cell cycle and other genes.

Introduction

Thymocyte selection-associated HMG-box protein (TOX) is a DNA-binding protein with essential roles in lymphocyte development and function. TOX is required for development of the $CD4^+$ T cell lineage in the thymus, and development of most innate lymphoid cell subsets in the bone marrow (1-4). While TOX is not expressed in most naive T cells, its expression induces and enforces a developmental exhaustion program in $CD8^+$ T cells experiencing chronic antigen exposure (5-7). Exhausted T cells have decreased cytotoxic

Corresponding Author: Jonathan Kaye, kayej@csmc.edu, phone: (310) 248-6541, fax: (310) 248-6650.

Author contributions: A.Y. and J.K. designed the project. A.Y., A.V., Z.Z, M.N., and B.S. performed the experiments. B.B. provided technical assistance. A.Y. analyzed the data and wrote the manuscript with contribution from J.K. and A.V. M.N. contributed to manuscript editing. All authors read and approved the final manuscript.

function, develop at the expense of memory cell formation, and are a major barrier to immune system control of tumors and chronic infections. While there has been much recent interest in TOX function, very little is known about TOX at the protein level.

We show here that the *Tox* gene encodes two proteins, despite a single mRNA. Mechanistically, the diversification of the TOX protein occurs via an alternative translation mechanism known as leaky ribosomal scanning. We also find that in a model of chronic stimulation of $CD8^+$ T cells leading to phenotypic exhaustion, over expression of the long form of TOX induces the expression of a unique gene set associated with regulation of the cell cycle.

Materials and Methods

Mice

OTI (C57BL/6-Tg(TcraTcrb)1100Mjb/J) mice and OTII (B6.Cg-Tg(TcraTcrb)425Cbn/J) mice were bred at Cedars-Sinai Medical Center or ordered from The Jackson Laboratory (Bar Harbor, ME) and kept under specific pathogen-free conditions. Mice used for experiments were 4-12 weeks of age and of either sex, with the exception of OTII mice which were solely males as the transgene integrated on the Y-chromosome. All animal procedures were performed in accordance with protocols approved by the Cedars-Sinai Medical Center Institutional Animal Care and Use Committee.

Generation of mutants

Mutant constructs were generated using the Invitrogen GeneArt Site-Directed Mutagenesis kit or the Agilent QuickChange II XL Site-Directed Mutagenesis (Santa Clara, CA) according to manufacturer's instructions. HEK293T or HEK293F cells were transfected using Xtreme Gene HD (Roche) or Fugene HD (Promega) at a 1:3 plasmid DNA to reagent ratio.

Flow cytometry and antibodies

Cell sorting was conducted by the Cedars Sinai Flow Cytometry core on a BD Aria III or Aria II, and FACS analysis performed on a LSRII (BD Biosciences, La Jolla, CA). Antibodies against TOX (TXRX10), CD4, CD8, CD3e, CD69, TIGIT, and LAG3, were from ThermoFisher Scientific (San Diego, CA), anti-Histone3 was from Cell Signaling Technology (Danvers, MA), and anti-PD1, isotype control, and Zombie live/dead stain were from BioLegend (San Diego, CA). The polyclonal TOX_{FL} antibody was raised against the N-terminal peptide sequence (MDVRFYPPPAQPAAAPAAPC) and produced by ProSci (Poway, CA). Data analysis was completed with FlowJo version 10 software (BD, Ashland, Oregon).

In vitro exhaustion assay

Chronic stimulation of $CD8^+$ T cells in culture was performed as described (8). Briefly, on day 0, naïve $CD8^+$ T cells were obtained via negative selection of OTI splenocytes using the EasySep Mouse Naïve $CD8^+$ T cell Isolation Kit (STEMCELL Technologies, Vancouver, BC). Cells were cultured in RPMI 1640, Pen/Strep/Glutamine, 1% HEPES, 1% 100 mM

Sodium Pyruvate, 1% NEAA (all Gibco, ThermoFisher Scientific, San Diego, CA), 10% FBS (Omega Scientific), 0.05 mM β-Mercaptoethanol (Sigma-Aldrich, St. Louis, MO), 5 ng/mL IL-7 (Peprotech, Cranbury, NJ), and 5 ng/mL IL-15 (BioLegend, San Diego, CA). Treatment groups included naïve, acutely stimulated, and chronically stimulated cells. Naïve cells were cultured in complete media only. Acutely stimulated cells were treated on Day 0 with 10 ng/mL $OVA_{(257-264)}$ peptide (Sigma-Aldrich, St. Louis, MO), washed on day 2, and cultured until day 5 in complete media. Chronically stimulated cells were treated with 10 ng/mL OVA peptide on days 0 and 1, washed on day two, and treated with OVA days 2-4 (total of 5 stimulations). All cells were collected day 5 for analysis.

TOX proteoform in vitro exhaustion assay

Retroviral constructs were created by insertion of TOX, M1T, or M(40,42,44)I sequences into p-MIG-eGFP retroviral vectors. Platinum-E Retroviral Packaging Cells (Cell Biolabs, Inc., San Diego, CA) were transfected in a 100 mm dish using Fugene HD Transfection Reagent (Promega, Madison, WI) with 10μgs of plasmid DNA. Viral supernatant was collected after 48 hours. On day 0, naïve $CD8^+$ T cells were obtained via negative selection of OTI splenocytes and cultured in complete RPMI with IL-7, IL-15, and OVA peptide as above. 24 hours later, cells were washed, and resuspended in viral supernatant supplemented with IL-7, IL-15, and 8 μg/mL polybrene (Sigma-Aldrich, St. Louis, MO). Cells were spin infected at 34°C for 75 minutes at 2000xg. Cells were returned to the incubator for 4 hours, washed, and resuspended in complete media with cytokines and OVA as above. Cells were treated with OVA again on day 2, media was changed on day 3, and cells collected for analysis on day 5.

Western blots

Whole cell lysates were made in RIPA buffer containing Pierce HALT Protease and Phosphatase Inhibitors (ThermoFischer Scientific, San Diego, CA). For T cells, 250,000 cell equivalents were loaded into each well. For HEK293F lysates, 10 ug of protein was loaded. Lysates were resolved by SDS-PAGE and transferred onto nitrocellulose membranes using the Transblot Turbo Transfer System (BioRad, Hercules, CA). Membranes were incubated in 5% milk TBST and incubated with primary antibodies overnight. Target proteins were visualized with appropriate HRP-conjugated secondary antibodies (ThermoFisher Scientific, San Diego, CA) and Pierce ECL Western Blotting Substrate (ThermoFisher Scientific, San Diego, CA). Blots were imaged and analyzed using a ChemiDoc XRS (BioRad, Hercules, CA) system.

Cell-free protein expression

The *Tox* gene was cloned into pSP64 Poly(A) Vector (Promega, Madison, WI), and protein produced using the TNT SP6 High-Yield Wheat Germ Protein Expression System (Promega, Madison, WI) according to manufacturer instructions.

RNA-seq analysis

Raw sequencing data was demultiplexed and converted to fastq format by using bcl2fastq v2.20 (Illumina, San Diego, California). Reads were aligned to the transcriptome using

STAR (version 2.6.1) / RSEM (version 1.2.28) with default parameters, using a custom mouse GRCm38 transcriptome reference downloaded from http://www.gencodegenes.org, containing all protein coding based on mouse GENCODE version 24 annotation (9, 10). Expression counts for each gene in all samples were normalized by a modified trimmed mean of the M-values normalization method. Each gene was fitted into a negative binomial generalized linear model, and the Wald test was applied to assess the differential expressions between two sample groups by DESeq2 (version 1.26.0) (11). Benjamini and Hochberg procedure was applied to adjust for multiple hypothesis testing, and differential expression gene (DEG) candidates were selected with a false discovery rate less than 0.05. DEG candidates were used for GO/KEGG enrichment analysis performed with ClusterProfileR (12).

Statistics

Means, one-way ANOVAs, and the p-value associated with a post-hoc Tukey's test was conducted for groups of three or more. *P* values of <0.05 were considered to represent means with a statistically significant difference (throughout all Figures, *$p<0.05$, ** $p\leq0.01$, *** $p\leq 0.001$). Sample or experiment sizes were determined empirically for sufficient statistical power. Outliers were identified using the interquartile range rule with a 1.5 constant.

Results

A N-terminally truncated TOX proteoform arises via internal translation initiation

The annotated *Tox* coding sequence is predicted to produce a 526 amino acid (a.a.) protein (TOX_{FL}) (13). However, when the annotated cDNA is introduced into HEK293 cells, which do not endogenously express TOX, western blots reveal two bands using a monoclonal antibody specific for the C-terminus of murine TOX (amino acids 336-526) (Fig. 1a). The proteoforms are not alternatively spliced variants, as both forms arise from a single cDNA and no cryptic splice sites have been identified. Previous studies (not shown) also failed to identify post-translational modifications that could account for such a large shift in electrophoretic mobility. Thus, we hypothesized the faster migrating band represented a truncated proteoform.

Alternative protein translation initiation is an important generator of proteome diversification. In healthy eukaryotic cells, most mRNAs are translated canonically, by a scanning-dependent mechanism that requires the presence of a 5' N7-methylated guanosine (m^7G) cap (14, 15). The 5' m^7G cap also functions as the recruitment site for the 40s ribosomal subunit, a methionine-conjugated initiator tRNA, and a host of eukaryotic initiation factors (eIFs) that comprise a translation "pre-initiation complex" (PIC). Inherent variability in the 5' untranslated region requires the small ribosomal subunit to proceed in the 5' to 3' direction base by base, scanning the mRNA until it recognizes an AUG start codon. Although the most 5' AUG is often the favored start codon, the sequence surrounding these initiation codons (Kozak sequence) affects the efficiency of initiation by eukaryotic ribosomes (16, 17).

The murine *Tox* mRNA coding sequence contains three downstream AUG codons (nucleotide positions 118-120 encoding methionine (M) 40, 124-126 encoding M42, and 130-132 encoding M44) that could potentially act as downstream translation start sites. Translation at these sites would produce N-terminally truncated proteins 487, 485, and 483 amino acids in length (Fig. 1b). Significantly these AUGs are also conserved in human and zebrafish TOX genes, consistent with functional and/or structural importance of the encoded residues (Fig. 1c). The apparent molecular weight (MW) change of the two TOX forms by western blot is also generally consistent with a loss of ~40-50 amino acids.

Based on these observations, we investigated whether the slower migrating protein band was TOX_{FL} translated from the annotated coding sequence TIS (TIS_{CDS}), and the faster migrating band a N-terminally truncated proteoform produced by internal translation. In this regard, we utilized site-directed mutagenesis to create a series of TOX mutant plasmids, which we introduced into HEK293F cells and analyzed the expressed proteins by western blot (Figs. 1a, d). Elimination of the annotated start codon by mutating the cDNA from ATG to ACG, encoding a threonine (M1T), specifically eliminated expression of the higher MW band (Fig. 1a, e). When the TIS_{CDS} was present but codons encoding M40, M42, and M44 were all mutated to encode isoleucine or glycine, only the higher MW band was detected (Fig. 1a, e). Therefore, we conclude that TOX_{FL} is translated from TIS_{CDS}, and the faster migrating proteoform (hence termed TOXΔN) is alternatively translated from an internal AUG.

To ensure TOXΔN production is not dependent on the presence of TOX_{FL} or the upstream nucleotide sequence (with exception of those required for the M40 Kozak sequence), we created two additional mutants to eliminate TOX_{FL} without eliminating the TIS_{CDS} (Fig. 1d). With a deletion-induced frameshift mutation at the R4 position, TOX_{FL} is not produced (although a 41 a.a. mutant protein could be translated from the TIS_{CDS}), but expression of TOXΔN is maintained, indicating the translation machinery does not require the TIS_{CDS} as context for downstream initiation (Fig. 1f, g). We further eliminated the possibility that TOXΔN is a post-translationally truncated proteoform of TOX_{FL} by mutating the C20 position to a stop codon. This eliminated production of TOX_{FL}, but not TOXΔN (Fig. 1f, g). Finally, we produced an antibody specific for the TOX N-terminal peptide. This antibody detected only TOX_{FL} (Fig. 1h).

TOXΔN proteoform is alternatively translated via leaky scanning

Internal translation initiation of a single reading frame could result from scanning-independent or scanning-dependent mechanisms. In terms of the former, mRNA secondary and tertiary structures can recruit the ribosome directly to an internal site (internal ribosome entry site, IRES) (18). Alternatively, scanning dependent mechanisms include ribosome re-initiation, TISU (Translation Initiator of Short 5' UTR)-mediated translation, and leaky ribosomal scanning. Ribosome re-initiation is unlikely as it most commonly occurs on mRNAs that utilize short upstream open reading frames to regulate the translation of the downstream product (19-21). Additionally, the *Tox* gene lacks a TISU (22). Given the potential for alternative in-frame starts in a single ORF in *Tox*, leaky ribosomal scanning remained a likely possibility (23).

To definitively distinguish scanning dependent translation and IRES-mediated translation of TOXΔN, we inserted a 48-base pair stable stem and loop structure 5' of the TIS_{CDS} in a TOX expression plasmid (Fig. 2a) (24). This plasmid also expresses EGFP downstream of an IRES sequence (Fig. 2a). Complex secondary mRNA structures are sterically blocked from entering the mRNA channel on the solvent side of the small ribosomal subunit, preventing progression of the ribosome, and thus would be expected to inhibit expression of TOX_{FL} (25, 26). HEK293F cells expressing TOX, the TOXΔN mutant, and the hairpin mutant had similar expression EGFP by FACS, consistent with IRES-mediated translation of the fluorescent reporter (Fig. 2b). In contrast, protein expression of TOX_{FL} was inhibited by the hairpin, as expected by scanning-dependent translation (Fig. 2c). However, the hairpin also inhibited expression of TOXΔN, demonstrating that its translation was also scanning-dependent and not IRES-mediated (Fig. 2c).

Leaky scanning occurs when the most 5' TIS is embedded in a Kozak sequence of reduced efficiency (16, 27). When sampled, the PIC can either initiate at the suboptimal TIS, or scan past it ("leak") and initiate at a downstream site. As such, the most proximal start site is typically highly efficient in order to prevent leaky scanning (27). Recently, Noderer et al. determined the translation initiation efficiency for all possible AUG initiation sequences in mammalian cells with an approach combining FACS and high-throughput DNA sequencing of a reporter library (17). They determined the high-efficiency initiation motif as RYMRMV**AUG**GC, where M = A or C and V =A, C, or G (17). Utilizing their data, we determined the efficiency of each TIS contained in *Tox* (Fig. 3a) (17). Consistent with the potential for leaky scanning, the Kozak sequences surrounding M40 and M44 were predicted to be more efficient than the M1 TIS_{CDS}, while M42 was predicted to be the least efficient (Fig. 3a). When we mutated the Kozak sequence surrounding M1 to be more efficient, which would be predicted to reduce leaky scanning, expression of TOXΔN was reduced (Fig. 3a-c). Changing the M1 TIS_{CDS} to a Kozak sequence of an equivalent strength did not significantly alter the ratio of the proteoforms (Fig. 3b, c).

Although the highly efficient M40 is the likely natural translational start for TOXΔN, a scanning mechanism would be predicted to utilize a downstream AUG in its absence. Thus, we tested the effect of various combinations of mutations of the downstream potential starts (M40G; M(42,44)G; M(40,44)I (Fig. 3d). Consistent with leaky scanning, translation of TOXΔN still occurs when M40 is eliminated (Fig. 3e, f). Eliminating both of the high efficiency initiation sites (M(40,44)I mutant) resulted in lower translation of TOXΔN compared to the other mutants, demonstrating that the efficiency of the TISs indeed regulates amounts of proteoform production (Fig. 3e, f). Interestingly, the N-terminus of TOX_{FL} is highly conserved in some forms of the TOX family genes TOX2 and TOX3, and those forms contain potential downstream initiation sites at a similar position to those in TOX (Fig. S1). The M1s from TOX2 and TOX3 have a similar efficiency score to TOX M1. However, the TOX2 downstream methionine (M43) has an equivalent efficiency to TOX2 M1. TOX3, in contrast, has two downstream methionines with M38/M39 (mouse/human) having a higher efficiency score than M1, a more favorable configuration for leaky scanning (Fig. S1). However, the contribution of these conserved sequences to the regulation of translation remains to be determined, especially considering the myriad of reported

transcripts that indicate that *Tox2* and *Tox3* loci may utilize other protein diversification mechanisms.

Leaky scanning of Tox mRNA is regulated at the cellular level

To determine whether the efficiency of leaky scanning is entirely dependent on the mRNA sequence or whether also regulated by the cellular context, we utilized an *in vitro* wheat germ lysate-based transcription-translation system expressing TOX under the control of an SP6 promoter. Surprisingly, this yielded only TOX_{FL} (Fig. 4a). Leaky scanning may not be favored in this highly efficient system due to specific eIF composition. But this also suggested that TOX proteoform expression might be a regulated process and highly dependent on cellular context.

To address this, we analyzed proteoform production during positive selection of CD4 T cells in the thymus, a TOX dependent process. Western blots of lysates from OTII TCR-transgenic thymocyte subpopulations show that the ratio of TOX proteoforms is indeed regulated during positive selection. Expression of TOX is low in pre-selection $CD4^+8^+$ (double positive, DP) thymocytes and favors expression of TOX_{FL} (Fig. 4b-d). TOX is upregulated as positive selection precedes, with peak expression in $CD4^+8^{lo}$ transitional cells (Fig. 4c), where lineage commitment occurs. This transition is accompanied by a switch to favoring TOXΔN over expression of TOX_{FL} (Fig. 4c, d). TOXΔN remains predominant as overall TOX expression declines in $CD69^+$ $CD4^+8^-$ (CD4SP) cells.

TOX also acts as an oncogenic factor in a number of hematological malignancies, including T cell acute lymphoblastic leukemia (T-ALL) (33) and cutaneous B and T cell lymphoma, particularly in the mycosis fungoides and Sézary syndrome subtypes (28-32). We found corresponding tumor cell lines also produce varying ratios of TOX forms (Fig. S2). Lysates from cutaneous T cell lymphoma derived HH cells, Sézary Syndrome derived Hut78 cells, T-ALL derived Molt4s, and Raji cells from a B cell lymphoma, were analyzed by western blot for TOX. Hut78 cells expressed more TOXΔN while the other cells lines produce more TOX_{FL}. Together, these data demonstrate that while the intrinsic efficiency of Kozak sequences controls the potential for leaky scanning, the particular cellular context regulates the quantitative pattern of TOX proteoform formation.

TOX_{FL} and TOXΔN have differing effects on $CD8^+$ T cell chronic stimulation

Chronic TCR-mediated stimulation induces sustained expression of TOX which is required to induce many features of CD8 T cell exhaustion (5, 7, 33, 34). This can be modeled in culture, where repeated stimulation of OVA-specific TCR transgenic OTI $CD8^+$ T cells leads to an exhausted phenotype (Fig. 5a) (8). Indeed, chronically but not acutely stimulated T cells in this system highly upregulate TOX and PD1, hallmarks of *in vivo* exhausted CD8 T cells (Fig. 5a). Interestingly, the ratio of proteoforms of TOX in chronically stimulated $CD8^+$ T cells was similar to pre-selection DP thymocytes, and lacked the predominance of TOXΔN as seen in thymocytes undergoing positive selection (Fig. S3a).

We took advantage of this system to ask if the individual forms of TOX could substitute for chronic stimulation. Naïve $CD3^+CD8^+$ splenocytes were isolated from OTI mice and stimulated with OVA peptide for 3 days to drive initial proliferation of the cells and allow

retroviral transduction. As this was insufficient to fully induce an exhausted phenotype, cells were also transduced to express TOX_{FL} or TOXΔN (and IRES-GFP) at 24 hours after initiation of culture to sustain TOX expression (Fig. 5b). Interestingly, using GFP expression as a surrogate marker for TOX expression, both long and short forms of TOX quantitatively induced PD1 and Tigit at roughly equivalent levels (Fig. S3b, c).

As known cell surface markers of the exhausted phenotype are limited, we also compared isolated GFP^- (exogenous TOX^-) and the top 20% of GFP^+ (exogenous TOX^+) populations by RNA-seq. Differentially expressed gene (DEG) analysis was performed, comparing GFP^+ cells from TOX_{FL} or TOXΔN cultures with GFP^- counterparts. Cells expressing exogenous TOX_{FL} contained a much higher number of DEGs than cells expressing TOXΔN (Fig. 5c). DEGs of note specifically regulated by TOX_{FL} but not TOXΔN include upregulated activation marker *Kit*, and downregulation of effector and memory associated genes including *Bhlhe40*, *Klf2*, and its target *S1pr1* (35-37). Pathway analysis of specific TOX_{FL} DEGs (adjusted p-value ≤ 0.05, and fold-change ≥2) showed enrichment for genes involved in the cell cycle and DNA replication, most of which were upregulated (Fig. 5d, e). Other significant pathways identified were the FOXO pathway and lysine degradation, which were overall downregulated.

Of the DEGs, two genes altered by both TOX_{FL} and TOXΔN, *Vipr1* and *Tubb6*, were previously reported as direct *Tox* gene targets in $CD8^+$ T cells by ChIP-seq (Fig. 5f) (34). Additionally, the gene target *Lrrk1* was also identified in $CD8^+$ T cells by ChIP-seq, but was only differentially expressed by mRNA in our samples expressing TOX_{FL} (Fig. 5c) (34). While no direct known gene targets were identified as unique to the TOXΔN sample, *Batf3* was predicted to be a binding site by expression of TOX fused to bacterial DNA adenine methyltransferase combined with deep sequencing (DAMID-Seq) (38). Thus, we conclude that both forms of TOX are transcriptionally active, likely contribute to T cell exhaustion, and regulate overlapping but distinct gene targets in isolation. However, TOX_{FL} has greater influence over the transcriptional landscape during chronic stimulation in culture.

Discussion

Here we described the mechanism of diversification of the TOX protein via an alternative translation mechanism known as leaky ribosomal scanning. This is due to a less than optimal Kozak sequence surrounding M1, leading to production of two distinct TOX proteins from a single mRNA. The *Tox* locus is not unique in this regard. Deep sequencing of ribosome-protected mRNA fragments allows for quantitative measuring of protein synthesis and ability to detect translation initiation sites at the codon level (39, 40). Studies utilizing permutations of this technique have revealed widespread usage of alternative TISs, including those that encode unannotated products from upstream open reading frames, amino-terminal truncations and extensions, out-of-frame products, and use of near cognate start codons (27, 39). In fact, ribosome profiling and N-terminal mass spectrometry estimate approximately 20% of human and mouse genes produce N-terminally truncated proteoforms via translation from internal start sites (41). It is interesting that not only M40, the likely downstream translational start based on Kozak efficiency and a 5’ to 3’ scanning mechanism, but also nearby downstream M42 and M44 are evolutionarily conserved. Whether these help to

ensure efficient TOXΔN production and/or are important structural element of the TOX protein remains to be determined. Likewise, whether the first 40 amino acids of TOX_{FL} serve as a structural or functional domain requires more investigation.

Thymic positive selection was associated not only with an increase in TOX expression, but also a switch to favoring TOXΔN production. As the mechanisms involved are not likely to be TOX-specific, this suggests that global changes in the control of translation site selection have the potential to be an important regulatory mechanism during T cell development, allowing greater leaky scanning. Leaky scanning is in part regulated by eIFs, with the fidelity of start codon recognition governed by eIF1 and eIF5 antagonism (42, 43). Competition between eIF1 and eIF5 stabilize the stringency of start codon recognition, and eIF1 and eIF5 are also engaged in a regulatory feedback loop that not only controls global TIS stringency, but their own translation. Whether the complex interplay between eIF1 to eIF5 also regulates T cell development, and T cell function, remains to be determined.

Interestingly, TOXΔN does not predominate in chronically stimulated $CD8^+$ T cells, as it does in differentiating thymocytes. In some instances, alternative translation mechanisms evolved to ensure the production of essential proteins during times of stress, when canonical translation is globally downregulated. The metabolic stress $CD8^+$ tumor infiltrating lymphocytes experience alters translation by changing the balance of key nutrients in the cell (44-46). The metabolic changes induced by the tumor microenvironment or during chronic stimulation could also affect levels of leaky scanning and thus TOX proteoform expression, with as yet unknown consequences on gene expression.

We also found that PD1 and other markers of an exhausted phenotype are upregulated in the context of either form of TOX in previously activated cells, but whether this is dependent on initial upregulation of endogenous TOX in this system remains to be determined. The *Pdcd1* transcript had an average fold change of 1.6 in DEG analysis, but failed to reach significance using an adjusted *p* value. It is possible there are some non-transcriptional effects of TOX or alternatively, *Pdcd1* upregulation, which appears to be dependent on very high levels of TOX, may be less prominent in the heterogenous GFP^+ population used for bulk RNA-seq (Fig. S3b, c). Nevertheless, TOX_{FL} on its own had a greater effect on other gene regulation during the enforcement of a model of T cell exhaustion than did TOXΔN. This is consistent with the maintenance of greater expression of TOX_{FL} in chronically stimulated T cells as compared to some thymocyte subpopulations. The data also indicate that the two forms of TOX may have distinct if somewhat overlapping roles in gene regulation. As both forms of TOX contain the identical DNA-binding domain, C-terminal domain and the majority of the N-terminal domain, it remains to be seen how the N-terminal peptide might influence TOX function. The N-terminal sequence is also highly conserved in some proteoforms of TOX family members TOX2 and TOX3, consistent with functional or structural importance. It is also possible that the two forms of TOX act synergistically to control cell fate, as we have not observed expression of one form without the other in cells.

Cells over-expressing TOX_{FL} uniquely upregulated cell cycle genes. TOX also controls the hierarchical development from proliferative progenitor-like state to one of terminal exhaustion in conjunction with TCF1 and T-bet (47). The induction of cell cycle

genes induced by TOX_{FL} may mimic this developmental process. As both resident and proliferating progenitor exhausted cells express TOX, it would be interesting to know whether the conversion to proliferating cells is driven by TOX_{FL}. Additionally, TOX expression has been shown to drive oncogenesis in T-ALL by altering the cell cycle and inducing proliferation of the tumor cells (33). The downregulation of *FoxO3, Klf2, S1pr1* and other FoxO signaling genes by TOX_{FL} is also intriguing. While the FoxO family plays significant roles in T cell homeostasis and differentiation, *FoxO3* has been shown to limit proliferation and promote the apoptosis of T cells during infection (48). Both of these findings are consistent with the requirement for TOX in the survival of exhausted $CD8^+$ T cells (6, 49).

Exhausted T cells are a major barrier to immune system control of tumors and chronic infections and prevention of their development and re-invigoration of existing exhausted cells is a major goal of immunotherapies. As knockdown of TOX improves T cell function in tumors and infection, it could be a viable pharmaceutical target (5-7, 50). This work helps ensure future studies are seeing the whole of TOX.

Supplementary Material

Refer to Web version on PubMed Central for supplementary material.

Acknowledgements

We would like to thank the Cedars-Sinai Medical Center Flow Cytometry and Applied Genomics core facilities for their expert technical assistance.

This research was supported by NIH grant R01AI054977 awarded to J.K.

Abbreviations used:

TOX	Thymocyte selection-associated HMG-box protein
m^7G	N7-methylated guanosine
eIF	eukaryotic initiation factor
PIC	pre-initiation complex
MW	molecular weight
AA	amino acid
TIS	translation initiation sequence
TIS_{CDS}	coding sequence TIS
IRES	internal ribosome entry site
TISU	Translation Initiator of Short 5’ UTR
T-ALL	T cell acute lymphoblastic leukemia

DEG	differentially expressed genes
dsM	downstream methionine

References

1. Seehus CR, Aliahmad P, de la Torre B, Iliev ID, Spurka L, Funari VA, and Kaye J. 2015. The development of innate lymphoid cells requires TOX-dependent generation of a common innate lymphoid cell progenitor. Nat Immunol 16: 599–608. [PubMed: 25915732]
2. Aliahmad P, Kadavallore A, de la Torre B, Kappes D, and Kaye J. 2011. TOX is required for development of the CD4 T cell lineage gene program. J Immunol Baltim Md 1950 187: 5931–40.
3. Aliahmad P, de la Torre B, and Kaye J. 2010. Shared dependence on the DNA-binding factor TOX for the development of lymphoid tissue-inducer cell and NK cell lineages. Nat Immunol 11: 945–52. [PubMed: 20818394]
4. Aliahmad P, and Kaye J. 2008. Development of all CD4 T lineages requires nuclear factor TOX. J Exp Medicine 205: 245–56.
5. Khan O, Giles JR, McDonald S, Manne S, Ngiow SF, Patel KP, Werner MT, Huang AC, Alexander KA, Wu JE, Attanasio J, Yan P, George SM, Bengsch B, Staupe RP, Donahue G, Xu W, Amaravadi RK, Xu X, Karakousis GC, Mitchell TC, Schuchter LM, Kaye J, Berger SL, and Wherry EJ. 2019. TOX transcriptionally and epigenetically programs CD8+ T cell exhaustion. Nature 571: 211–218. [PubMed: 31207603]
6. Alfei F, Kanev K, Hofmann M, Wu M, Ghoneim HE, Roelli P, Utzschneider DT, von Hoesslin M, Cullen JG, Fan Y, Eisenberg V, Wohlleber D, Steiger K, Merkler D, Delorenzi M, Knolle PA, Cohen CJ, Thimme R, Youngblood B, and Zehn D. 2019. TOX reinforces the phenotype and longevity of exhausted T cells in chronic viral infection. Nature 571: 265–269. [PubMed: 31207605]
7. Scott AC, Dündar F, Zumbo P, Chandran SS, Klebanoff CA, Shakiba M, Trivedi P, Menocal L, Appleby H, Camara SJ, Zamarin D, Walther T, Snyder AC, Femia MR, Comen EA, Wen HY, Hellmann MD, Anandasabapathy N, Liu Y, Altorki NK, Lauer P, Levy O, Glickman M, Kaye J, Betel D, Philip M, and Schietinger A. 2019. TOX is a critical regulator of tumour-specific T cell differentiation. Nature 571: 270–274. [PubMed: 31207604]
8. Zhao M, Kiernan CH, Stairiker CJ, Hope JL, Leon LG, van Meurs M, Brouwers-Haspels I, Boers R, Boers J, Gribnau J, van IJcken WFJ, Bindels EM, Hoogenboezem RM, Erkeland SJ, Mueller YM, and Katsikis PD. 2020. Rapid in vitro generation of bona fide exhausted CD8+ T cells is accompanied by Tcf7 promotor methylation. Plos Pathog 16: e1008555. [PubMed: 32579593]
9. Li B, and Dewey CN. 2011. RSEM: accurate transcript quantification from RNA-Seq data with or without a reference genome. Bmc Bioinformatics 12: 323. [PubMed: 21816040]
10. Dobin A, Davis CA, Schlesinger F, Drenkow J, Zaleski C, Jha S, Batut P, Chaisson M, and Gingeras TR. 2013. STAR: ultrafast universal RNA-seq aligner. Bioinformatics 29: 15–21. [PubMed: 23104886]
11. Love MI, Huber W, and Anders S. 2014. Moderated estimation of fold change and dispersion for RNA-seq data with DESeq2. Genome Biol 15: 550. [PubMed: 25516281]
12. Wu T, Hu E, Xu S, Chen M, Guo P, Dai Z, Feng T, Zhou L, Tang W, Zhan L, Fu X, Liu S, Bo X, and Yu G. 2021. clusterProfiler 4.0: A universal enrichment tool for interpreting omics data. Innovation 2: 100141. [PubMed: 34557778]
13. Wilkinson B, Chen JY-F, Han P, Rufner KM, Goularte OD, and Kaye J. 2002. TOX: an HMG box protein implicated in the regulation of thymocyte selection. Nat Immunol 3: 272–280. [PubMed: 11850626]
14. Hellen CUT 2018. Translation Termination and Ribosome Recycling in Eukaryotes. Csh Perspect Biol 10: a032656.
15. Aitken CE, and Lorsch JR. 2012. A mechanistic overview of translation initiation in eukaryotes. Nat Struct Mol Biol 19: 568–576. [PubMed: 22664984]
16. Kozak M 1986. Point mutations define a sequence flanking the AUG initiator codon that modulates translation by eukaryotic ribosomes. Cell 44: 283–92. [PubMed: 3943125]

17. Noderer WL, Flockhart RJ, Bhaduri A, de Arce AJD, Zhang J, Khavari PA, and Wang CL. 2014. Quantitative analysis of mammalian translation initiation sites by FACS-seq. Mol Syst Biol 10: 748. [PubMed: 25170020]
18. Sarnow P 2003. Viral Internal Ribosome Entry Site Elements: Novel Ribosome-RNA Complexes and Roles in Viral Pathogenesis. J Virol 77: 2801–2806. [PubMed: 12584303]
19. MEIJER HA, and THOMAS AAM. 2002. Control of eukaryotic protein synthesis by upstream open reading frames in the 5′-untranslated region of an mRNA. Biochem J 367: 1–11. [PubMed: 12117416]
20. Morris DR, and Geballe AP. 2000. Upstream Open Reading Frames as Regulators of mRNA Translation. Mol Cell Biol 20: 8635–8642. [PubMed: 11073965]
21. Calvo SE, Pagliarini DJ, and Mootha VK. 2009. Upstream open reading frames cause widespread reduction of protein expression and are polymorphic among humans. Proc National Acad Sci 106: 7507–7512.
22. Elfakess R, and Dikstein R. 2008. A Translation Initiation Element Specific to mRNAs with Very Short 5′UTR that Also Regulates Transcription. Plos One 3: e3094. [PubMed: 18769482]
23. Touriol C, Bornes S, Bonnal S, Audigier S, Prats H, Prats A-C, and Vagner S. 2003. Generation of protein isoform diversity by alternative initiation of translation at non-AUG codons. Biol Cell 95: 169–178. [PubMed: 12867081]
24. Babendure JR, Babendure JL, Ding J-H, and Tsien RY. 2006. Control of mammalian translation by mRNA structure near caps. Rna 12: 851–861. [PubMed: 16540693]
25. Pisarev AV, Kolupaeva VG, Yusupov MM, Hellen CU, and Pestova TV. 2008. Ribosomal position and contacts of mRNA in eukaryotic translation initiation complexes. Embo J 27: 1609–1621. [PubMed: 18464793]
26. Abaeva IS, Marintchev A, Pisareva VP, Hellen CUT, and Pestova TV. 2010. Bypassing of stems versus linear base-by-base inspection of mammalian mRNAs during ribosomal scanning: Ribosomal scanning on structured eukaryotic mRNAs. Embo J 30: 115–129. [PubMed: 21113134]
27. Ingolia NT, Lareau LF, and Weissman JS. 2011. Ribosome profiling of mouse embryonic stem cells reveals the complexity and dynamics of mammalian proteomes. Cell 147: 789–802. [PubMed: 22056041]
28. Huang Y, Su M-W, Jiang X, and Zhou Y. 2015. Evidence of an oncogenic role of aberrant TOX activation in cutaneous T-cell lymphoma. Blood 125: 1435–1443. [PubMed: 25548321]
29. Dulmage BO, Akilov O, Vu JR, Falo LD, and Geskin LJ. 2019. Dysregulation of the TOX-RUNX3 pathway in cutaneous T-cell lymphoma. Oncotarget 10: 3104–3113. [PubMed: 31139323]
30. Yu X, Luo Y, Liu J, Liu Y, and Sun Q. 2015. TOX acts an oncological role in mycosis fungoides. Plos One 10: e0117479. [PubMed: 25811617]
31. McGirt LY, Degesys CA, Johnson VE, Zic JA, Zwerner JP, and Eischen CM. 2016. TOX expression and role in CTCL. J Eur Acad Dermatol 30: 1497–1502.
32. Morimura S, Sugaya M, Suga H, Miyagaki T, Ohmatsu H, Fujita H, Asano Y, Tada Y, Kadono T, and Sato S. 2014. TOX expression in different subtypes of cutaneous lymphoma. Arch Dermatol Res 306: 843–9. [PubMed: 25216799]
33. Lobbardi R, Pinder J, Martinez-Pastor B, Theodorou M, Blackburn JS, Abraham BJ, Namiki Y, Mansour M, Abdelfattah NS, Molodtsov A, Alexe G, Toiber D, de Waard M, Jain E, Boukhali M, Lion M, Bhere D, Shah K, Gutierrez A, Stegmaier K, Silverman LB, Sadreyev RI, Asara JM, Oettinger MA, Haas W, Look AT, Young RA, Mostoslavsky R, Dellaire G, and Langenau DM. 2017. TOX Regulates Growth, DNA Repair, and Genomic Instability in T-cell Acute Lymphoblastic Leukemia. Cancer Discov 7: 1336–1353. [PubMed: 28974511]
34. Page N, Klimek B, Roo MD, Steinbach K, Soldati H, Lemeille S, Wagner I, Kreutzfeldt M, Liberto GD, Vincenti I, Lingner T, Salinas G, Brück W, Simons M, Murr R, Kaye J, Zehn D, Pinschewer DD, and Merkler D. 2018. Expression of the DNA-Binding Factor TOX Promotes the Encephalitogenic Potential of Microbe-Induced Autoreactive CD8+ T Cells. Immunity 48: 937–950.e8. [PubMed: 29768177]
35. Frumento G, Zuo J, Verma K, Croft W, Ramagiri P, Chen FE, and Moss P. 2019. CD117 (c-Kit) Is Expressed During CD8+ T Cell Priming and Stratifies Sensitivity to Apoptosis According to Strength of TCR Engagement. Front Immunol 10: 468. [PubMed: 30930902]

36. Salmon AJ, Shavkunov AS, Miao Q, Jarjour NN, Keshari S, Esaulova E, Williams CD, Ward JP, Highsmith AM, Pineda JE, Taneja R, Chen K, Edelson BT, and Gubin MM. 2022. BHLHE40 Regulates the T-Cell Effector Function Required for Tumor Microenvironment Remodeling and Immune Checkpoint Therapy EfficacyEffective Immune Checkpoint Therapy Requires BHLHE40. Cancer Immunol Res 10: 597–611. [PubMed: 35181783]
37. Skon CN, Lee J-Y, Anderson KG, Masopust D, Hogquist KA, and Jameson SC. 2013. Transcriptional downregulation of S1pr1 is required for the establishment of resident memory CD8+ T cells. Nat Immunol 14: 1285–1293. [PubMed: 24162775]
38. de J.Domingues AM, Artegiani B, Dahl A, and Calegari F. 2016. Identification of Tox chromatin binding properties and downstream targets by DamID-Seq. Genom Data 7: 264–8. [PubMed: 26981424]
39. Ingolia NT, Ghaemmaghami S, Newman JRS, and Weissman JS. 2009. Genome-wide analysis in vivo of translation with nucleotide resolution using ribosome profiling. Sci New York N Y 324: 218–23.
40. Lee S, Liu B, Lee S, Huang S-X, Shen B, and Qian S-B. 2012. Global mapping of translation initiation sites in mammalian cells at single-nucleotide resolution. Proc National Acad Sci 109: E2424–E2432.
41. Damme PV, Gawron D, Criekinge WV, and Menschaert G. 2014. N-terminal Proteomics and Ribosome Profiling Provide a Comprehensive View of the Alternative Translation Initiation Landscape in Mice and Men. Mol Cell Proteomics 13: 1245–1261. [PubMed: 24623590]
42. Pestova TV, and Kolupaeva VG. 2002. The roles of individual eukaryotic translation initiation factors in ribosomal scanning and initiation codon selection. Gene Dev 16: 2906–22. [PubMed: 12435632]
43. Ivanov IP, Loughran G, Sachs MS, and Atkins JF. 2010. Initiation context modulates autoregulation of eukaryotic translation initiation factor 1 (eIF1). Proc National Acad Sci 107: 18056–18060.
44. Bengsch B, Johnson AL, Kurachi M, Odorizzi PM, Pauken KE, Attanasio J, Stelekati E, McLane LM, Paley MA, Delgoffe GM, and Wherry EJ. 2016. Bioenergetic Insufficiencies Due to Metabolic Alterations Regulated by the Inhibitory Receptor PD-1 Are an Early Driver of CD8+ T Cell Exhaustion. Immunity 45: 358–373. [PubMed: 27496729]
45. Schurich A, Pallett LJ, Jajbhay D, Wijngaarden J, Otano I, Gill US, Hansi N, Kennedy PT, Nastouli E, Gilson R, Frezza C, Henson SM, and Maini MK. 2016. Distinct Metabolic Requirements of Exhausted and Functional Virus-Specific CD8 T Cells in the Same Host. Cell Reports 16: 1243–1252. [PubMed: 27452473]
46. Ho P-C, Bihuniak JD, Macintyre AN, Staron M, Liu X, Amezquita R, Tsui Y-C, Cui G, Micevic G, Perales JC, Kleinstein SH, Abel ED, Insogna KL, Feske S, Locasale JW, Bosenberg MW, Rathmell JC, and Kaech SM. 2015. Phosphoenolpyruvate Is a Metabolic Checkpoint of Anti-tumor T Cell Responses. Cell 162: 1217–1228. [PubMed: 26321681]
47. Beltra J-C, Manne S, Abdel-Hakeem MS, Kurachi M, Giles JR, Chen Z, Casella V, Ngiow SF, Khan O, Huang YJ, Yan P, Nzingha K, Xu W, Amaravadi RK, Xu X, Karakousis GC, Mitchell TC, Schuchter LM, Huang AC, and Wherry EJ. 2020. Developmental Relationships of Four Exhausted CD8+ T Cell Subsets Reveals Underlying Transcriptional and Epigenetic Landscape Control Mechanisms. Immunity 52: 825–841.e8. [PubMed: 32396847]
48. Sullivan JA, Kim EH, Plisch EH, and Suresh M. 2012. FOXO3 Regulates the CD8 T Cell Response to a Chronic Viral Infection. J Virol 86: 9025–9034. [PubMed: 22675000]
49. Yao C, Sun H-W, Lacey NE, Ji Y, Moseman EA, Shih H-Y, Heuston EF, Kirby M, Anderson S, Cheng J, Khan O, Handon R, Reilley J, Fioravanti J, Hu J, Gossa S, Wherry EJ, Gattinoni L, McGavern DB, O'Shea JJ, Schwartzberg PL, and Wu T. 2019. Single-cell RNA-seq reveals TOX as a key regulator of CD8+ T cell persistence in chronic infection. Nat Immunol 20: 890–901. [PubMed: 31209400]
50. Kim K, Park S, Park SY, Kim G, Park SM, Cho J-W, Kim DH, Park YM, Koh YW, Kim HR, Ha S-J, and Lee I. 2020. Single-cell transcriptome analysis reveals TOX as a promoting factor for T cell exhaustion and a predictor for anti-PD-1 responses in human cancer. Genome Med 12: 22. [PubMed: 32111241]

Key Points

- A single *Tox* mRNA encodes 2 proteoforms with different N-termini.
- Truncated TOX is translated by leaky scanning and regulated by cell context.
- Alternative TOX proteins have overlapping but distinct effects on gene expression.

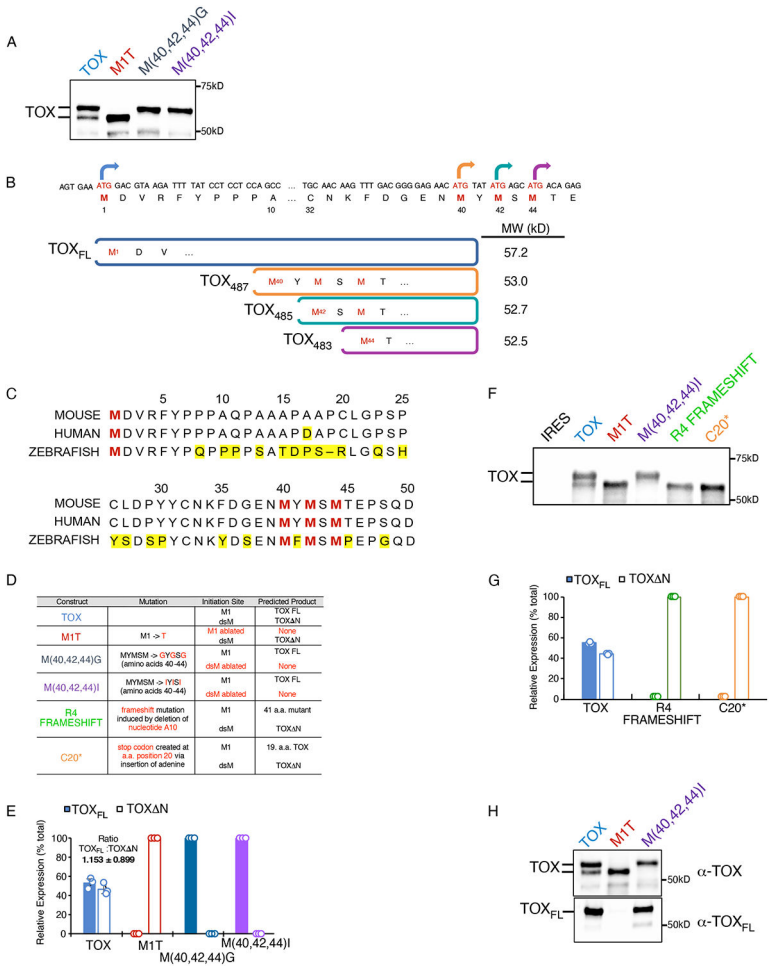

Figure 1.

The *Tox gene* encodes two proteins from a single mRNA. **(A)** Western blot of lysates from FACS sorted GFP$^+$ HEK293F cells expressing TOX and mutant proteins. Data are representative of three independent experiments. **(B)** Predicted N-terminally truncated proteins of 487, 485, and 483 amino acids in length could be produced from internal translation start sites. **(C)** The TOX protein contains evolutionarily conserved alternative translation start sites at positions M40, M42, and M44 **(D)** TOX mutants and predicted products described in the study. **(E)** Quantitation of protein forms as in **(A)**, with each band expressed as a percent of total. Not detected (N.D.) is indicated for some samples. Data are representative of three independent experiments (each group n=3). **(F)** Western blot of lysates from FACS sorted GFP$^+$ HEK293F cells expressing TOX and mutant proteins. **(G)** Quantitation of protein forms as in **(F)**, with each band expressed as a percent of total. Data are pooled from three independent experiments (each group n=3). **(H)** Western blot of HEK293F lysates expressing TOX and mutant proteins, probed with commercial monoclonal antibody (upper panel) or an N-terminal specific antibody (lower panel).

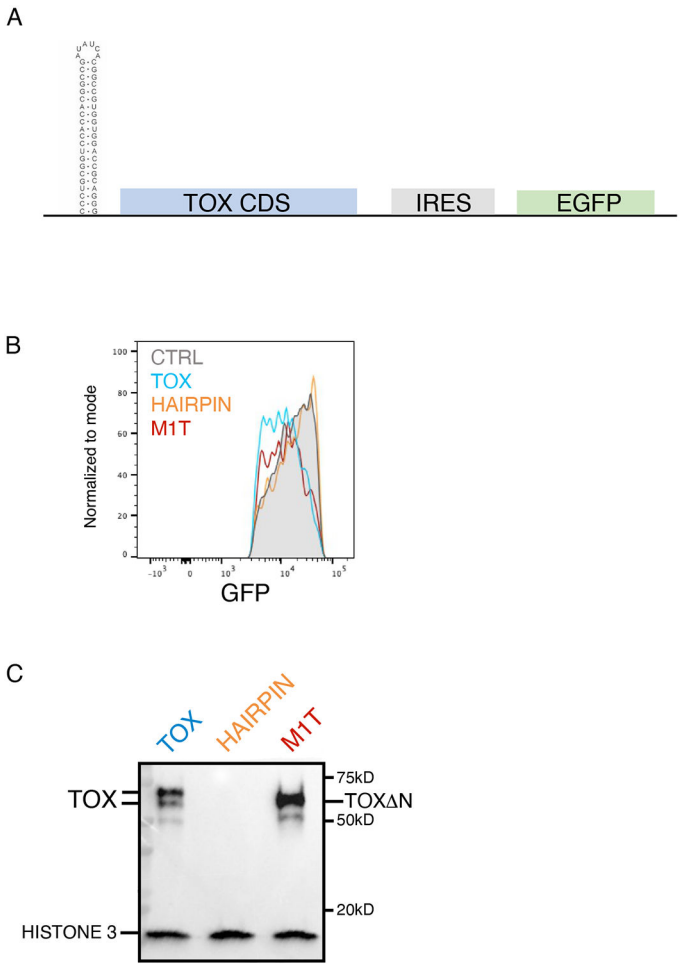

Figure 2.

TOX ΔN is translated via a scanning-dependent mechanism. **(A)** Schematic of hairpin plasmid encoding TOX and IRES-dependent EGFP. **(B)** FACS-analysis of GFP in HEK293F cells expressing TOX, M1T and hairpin TIS_{CDS} mutants. Representative of four independent experiments. **(C)** Expression of TOX by western blot in FACS-sorted GFP^{+} HEK293F cells expressing the indicated genes. Expression of histone 3 is shown as control. Representative of four independent experiments.

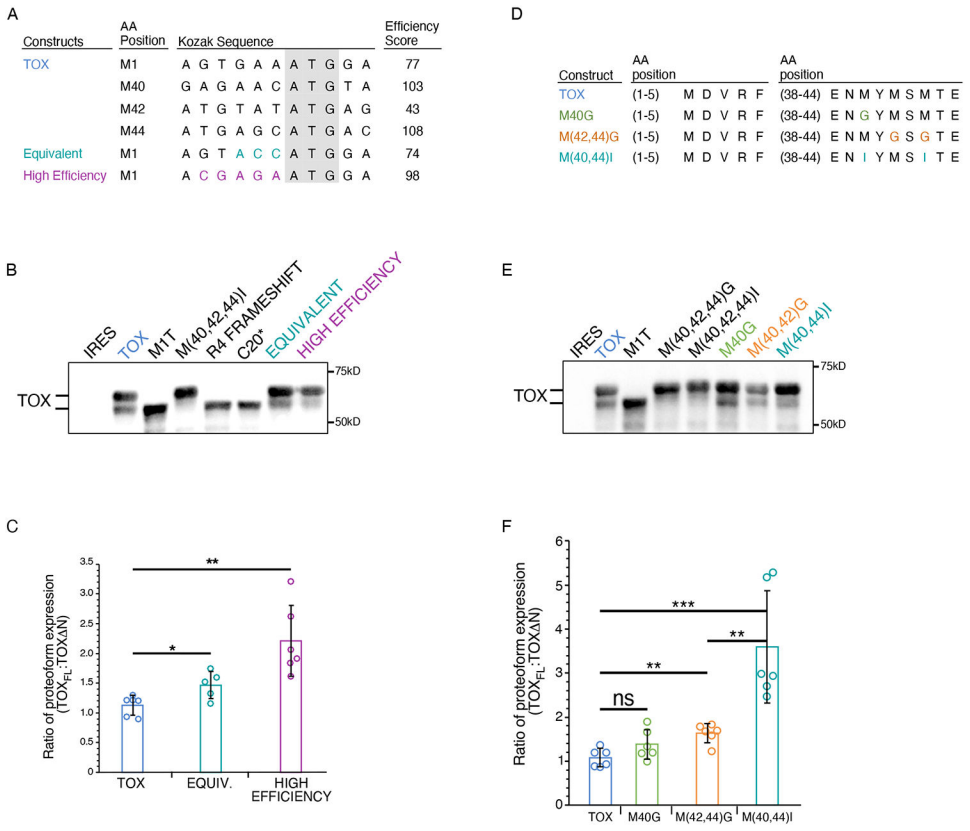

Figure 3.

TOX**Δ**N is alternatively translated via leaky scanning. **(A)** Predicted translation efficiency scores for each TIS in TOX or in mutants. **(B)** Western blot of lysates from FACS sorted GFP$^+$ HEK293F cells expressing TOX and mutant proteins. Data are representative of five to six independent experiments. **(C)** Relative quantification of data generated as in (B), expressed as the ratio of TOX_{FL} to TOX**Δ**N (TOX and High Efficiency n=6; Equivalent n=5). **(D)** Iterative mutations of the downstream starts (M40G; M(42,44)G; M(40,44)I). **(E)** Western blot of lysates from FACS sorted GFP$^+$ HEK293F cells expressing TOX and mutant proteins. Data are representative of six independent experiments. **(F)** Relative quantification expressed as the ratio of TOX_{FL} to TOX**Δ**N. Data are pooled from six independent experiments (each group n=6).

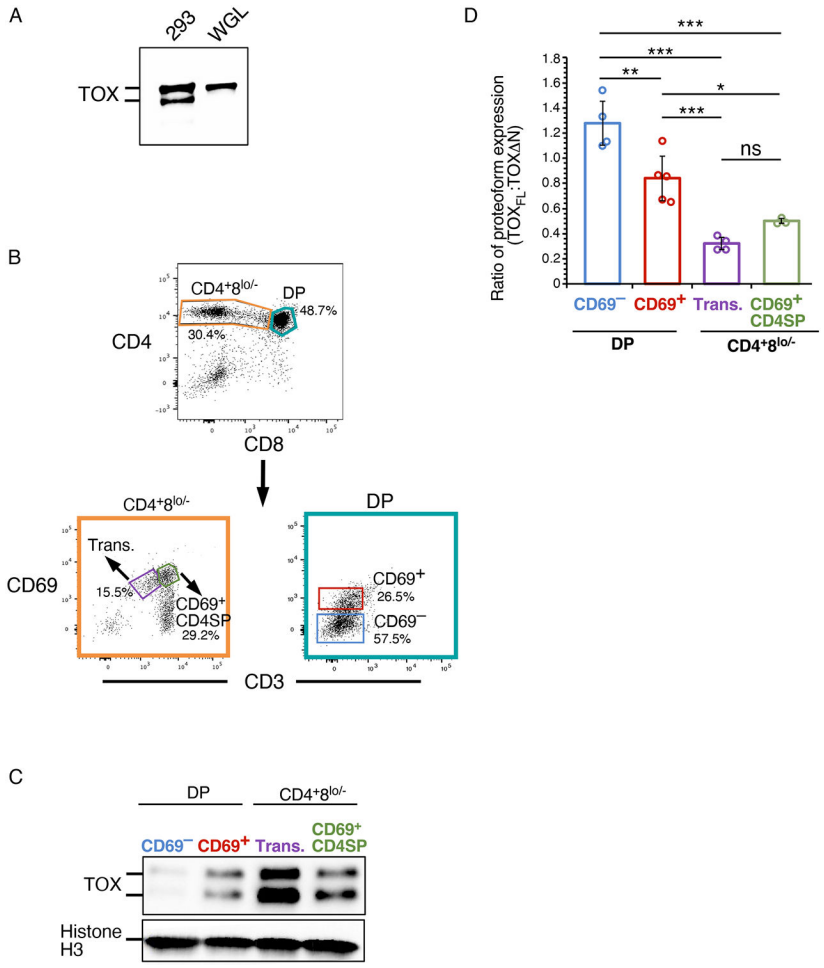

Figure 4.

Leaky scanning of TOX**Δ**N is a regulated process. **(A)** Western blot of lysate from HEK293 cells transfected with TOX or TOX expressed by wheat germ lysate in a cell-free transcription-translation system. Data is representative of 2 independent experiments. **(B)** Gating strategy for isolation of murine thymocytes from OTII transgenic mice: pre-selection or post-selection DP ($CD4^+8^+$ $CD69^-$ or $CD69^+$, respectively); transitional cells ($CD4^+8^{lo}CD3^{int}CD69^+$); $CD69^+CD4SP$ ($CD4^+8^-CD3^{hi}CD69^+$) **(C)** Western blot of lysate from 250,000 cell equivalents. Data are representative of two pooled mice from three to five independent experiments. **(D)** Relative quantification of data generated as in (C), expressed as the ratio of TOX_{FL} to TOX**Δ**N ($CD4^+8^+$ $CD69^-$ and transitional n=4; $CD4^+8^+$ $CD69^+$ n=5; $CD69^+CD4SP$ n=3).

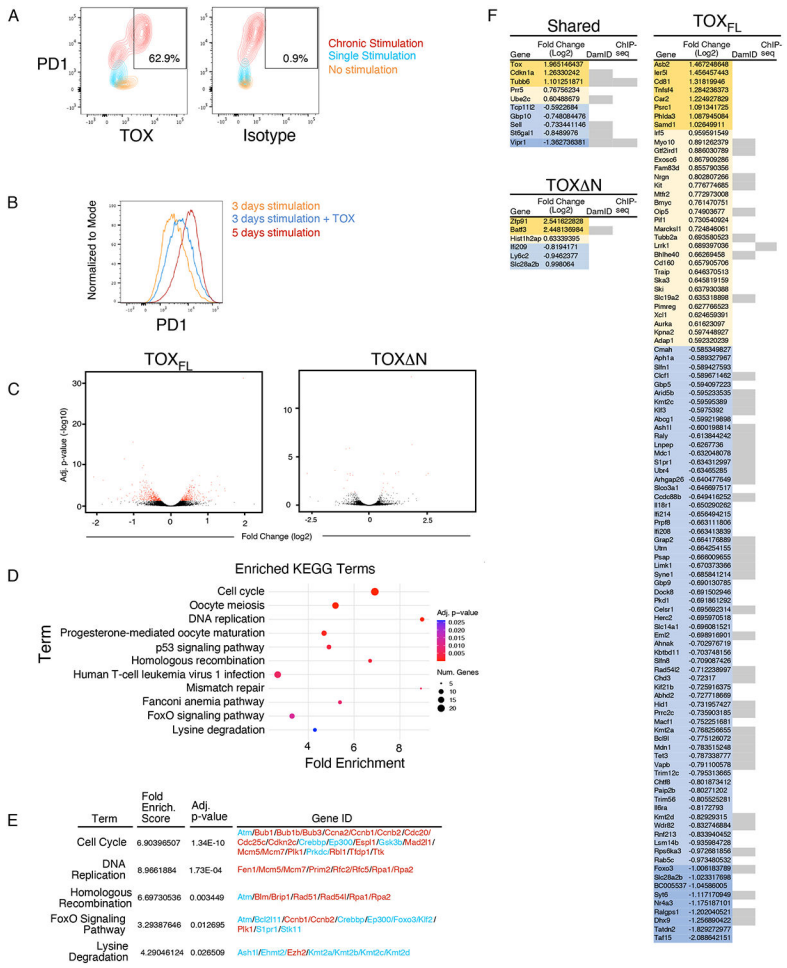

Figure 5.

TOX proteoforms induce differing gene expression in a model of CD8$^+$ T cell exhaustion. **(A)** FACS plots showing TOX and PD1 expression in naïve, singly stimulated, and chronically stimulated CD8$^+$ T cells. Data is representative of 5 independent experiments, using 2 pooled mice each. **(B)** FACS plots of PD1 expression in CD8$^+$ T cells stimulated 3 or 5 times with OVA, or three times with OVA and transduced to express TOX. Data is representative of two independent experiments using two pooled mice each. **(C)** RNA-seq was carried out in duplicate, using 2 pooled mice per condition. Expression of TOX_{FL} results in a greater number of significantly differentially expressed gene than expression of TOX**Δ**N as shown in volcano plots. **(D)** GO analysis terms for DEGs found in TOX_{FL} only. **(D/E)** TOX_{FL} upregulates genes associated with the cell cycle and DNA replication and downregulates those associated with FoxO signaling and lysine degradation. Upregulated genes shown in red, downregulated genes in blue. **(F)** List of DEGs found only in TOX_{FL}, only in TOX**Δ**N, or shared. Genes identified as potential TOX gene targets using published Dam-ID or ChIP-seq data are identified by corresponding grey bars.